ELSEVIER

Journal of Power Sources 73 (1998) 36–46

JOURNAL OF POWER SOURCES

Oxide for valve-regulated lead–acid batteries

L.T. Lam [a,*], O.V. Lim [a], N.P. Haigh [a], D.A.J. Rand [a], J.E. Manders [b], D.M. Rice [b]

[a] *CSIRO, Division of Minerals, P.O. Box 312, Clayton South, Victoria 3169, Australia*
[b] *Pasminco Metals, P.O. Box 1291K, Melbourne, Victoria 3001, Australia*

Received 18 June 1997; accepted 17 August 1997

Abstract

In order to meet the increasing demand for valve-regulated lead–acid (VRLA) batteries, a new soft lead has been produced by Pasminco Metals. In this material, bismuth is increased to a level that produces a significant improvement in battery cycle life. By contrast, other common impurities, such as arsenic, cobalt, chromium, nickel, antimony and tellurium, that are known to be harmful to VRLA batteries are controlled to very low levels. A bismuth (Bi)-bearing oxide has been manufactured (Barton-pot method) from this soft lead and is characterized in terms of phase composition, particle size distribution, BET surface area, and reactivity. An investigation is also made of the rates of oxygen and hydrogen evolution on pasted electrodes prepared from the Bi-bearing oxide. For comparison, the characteristics and performance of a Bi-free (Barton-pot) oxide, which is manufactured in the USA, are also examined. Increasing the level of bismuth and lowering those of the other impurities in soft lead produces no unusual changes in either the physical or the chemical properties of the resulting Bi-bearing oxide compared with Bi-free oxide. This is very important because there is no need for battery manufacturers to change their paste formulae and paste-mixing procedures on switching to the new Bi-bearing oxide. There is little difference in the rates of oxygen and hydrogen evolution on pasted electrodes prepared from Bi-bearing or Bi-free oxides. On the other hand, these rates increase on the former electrodes when the levels of all the other impurities are made to exceed (by deliberately adding the impurities as oxide powders) the corresponding, specified values for the Bi-bearing oxide. The latter behaviour is particularly noticeable for hydrogen evolution, which is enhanced even further when a negative electrode prepared from Bi-bearing oxide is contaminated through the deposition of impurities added to the sulfuric acid solution. The effects of impurities in the positive and negative plates on the performance of both flooded-electrolyte and VRLA batteries are assessed in terms of water loss, charge efficiency, grid corrosion, and self-discharge. Finally, the causes of negative-plate discharge in VRLA batteries under float conditions are addressed.

Keywords: Bismuth; Hydrogen evolution; Impurity; Lead–acid battery; Oxygen evolution; Soft lead

1. Background

The use of valve-regulated lead–acid (VRLA) batteries that require no water maintenance has rapidly become widespread. For stationary applications, in particular, these designs are replacing conventional, flooded-electrolyte batteries. There have also been several demonstrations [1–4] of the feasibility of VRLA batteries using absorptive glass-mat (AGM) separators for automotive service. It has been claimed that these batteries give competitive, or even better, results than either flooded, low-maintenance or flooded, maintenance-free designs [2,3]. For example, the performance of automotive VRLA batteries is equivalent to that of flooded-electrolyte designs with low-antimony (Pb–Sb) positive grids; but when both battery types use the same lead–calcium–tin (Pb–Ca–Sn) alloy for the positive grids, the cold-cranking and cycle-life capabilities of VRLA batteries are superior. A further market is opening up for VRLA batteries. In the early 1990s, the US Federal Government, together with some US State Governments, provided a new impetus for the development of an electric vehicle (EV) industry through legislation aimed at decreasing national petroleum dependence and reducing the impact of automotive emissions on the urban environment. VRLA batteries are considered widely to be the most practical power source for the near-term EV markets.

Since VRLA batteries with AGM separators employ lower volumes of sulfuric acid solution than flooded-electrolyte equivalents, the former technology generally operates under ‘acid-starved’ conditions. Accordingly, water loss during battery service must be kept to a minimum; otherwise, the battery will fail through electrolyte dry-out.

* Corresponding author.

0378-7753/98/$19.00

Oxygen and hydrogen evolution occur as side reactions during the charging process of lead–acid batteries. In a VRLA battery, however, the oxygen evolved from the positive plates diffuses through either the pores of the separators or the head space of the container to the negative plates where it is reduced back to water. By contrast, the hydrogen evolved from the negative plates cannot be oxidized (or rather can only be oxidized at a very low rate) back to water at the opposite positive plates. Thus, any hydrogen emission will translate to a permanent loss of water from the battery. Accordingly, minimization of the rates of both hydrogen and oxygen gassing, together with the promotion of efficient oxygen recombination, are important objectives in the design of VRLA batteries.

The gassing behaviour of VRLA batteries is influenced strongly by the composition/nature of the grid alloys (i.e., Pb–Sb vs. Pb–Ca–Sn), the levels of impurities (i.e., Sb, Ni, Co, Se, etc.) in the raw lead materials used to manufacture the positive and negative plates, and the charging conditions [5–7]. On the other hand, the efficiency of oxygen recombination depends on the degree of compression of the plate-group, the extent of electrolyte saturation of the glass–mat separators, and the action of certain minor elements in the negative mass, such as bismuth and tin [8,9]. These elements—especially bismuth [9]—have been found to promote the reduction of oxygen, and can also exert beneficial effects on the cycle life of both flooded-electrolyte and VRLA designs of lead–acid battery.

With respect to acceptable levels of impurities in the starting lead material, the majority of the present specifications set for soft lead have focused on battery technologies which are based on antimonial grid alloys. In these designs, the antimony in the positive and negative grids dominates the performance of the battery, and the influence of minor impurities is of little importance. For VRLA batteries that employ antimony-free grid alloys (i.e., Pb–Sn and/or Pb–Ca–Sn) there is, however, an urgent need to develop a more stringent specification for soft lead in order to exclude, or restrict adequately, those impurities which exert a deleterious effect on gassing performance. Based on research conducted both in a joint CSIRO–Pasminco research programme [9,10] and by other workers [8,11,12], Pasminco [13] has recently proposed a specification for soft lead to suit the requirements of VRLA batteries. In this new specification, impurities such as As, Co, Cr, Ni, Sb, and Te that are known to be harmful to VRLA batteries are limited to very low levels. By contrast, bismuth, which has been demonstrated as being beneficial, is increased to levels at which significant improvements in battery performance can be achieved.

Soft lead with the new specification has been produced by Pasminco and supplied to a domestic lead–acid battery company for conversion to Barton-pot oxide. CSIRO has undertaken a study of the physico-chemical characteristics of this oxide, together with an evaluation of its effects on both oxygen and hydrogen evolution. For the purpose of comparison, corresponding benchmark tests have also been conducted on oxide which contains virtually no bismuth (i.e., < 0.005 wt.%).

Table 1
Phase composition (wt.%) of Barton-pot oxide

Oxide type	Pb	α-PbO
Bi-bearing oxide	21	79
Bi-free oxide	27	73

2. Oxide characterization

Two Barton-pot oxides were examined in this study: one contains ~ 0.05 wt.% Bi and was produced from soft lead with the specifications proposed by Pasminco (termed 'Bi-bearing oxide'); the other oxide contains only trace amounts of bismuth (termed 'Bi-free oxide') and was supplied by a manufacturer in the USA. Phase-analysis data for these oxides are given in Table 1. The results show that both oxides consist of only lead and α-PbO. The Bi-bearing oxide has a slightly lower free-lead content, and thus a correspondingly higher proportion of α-PbO, than the Bi-free oxide. The absence of β-PbO indicates that the oxides have been prepared at a relatively low temperature.

The particle size distribution of the Bi-free and Bi-bearing oxides was determined with a Malvern Mastersizer S, Version 2.14, standard particle size analyzer. The results for the two oxides are very similar. The particle size distribution of the Bi-bearing oxide is given in Fig. 1. The oxide is composed of two types of particle: 'type 1' particles have sizes < 0.9 μm and 'type 2' particles have sizes > 1.1 μm. The most frequent diameter of the particles in types 1 and 2 is 0.3–0.4 μm and 6–8 μm, respectively. The distribution curve of type 1 particles is more symmetrical than that of type 2 particles. At large particle sizes, it appears that a third distribution overlaps the curve for type 2 particles. This is due to the presence of free-lead particles which, in a Barton-pot oxide, usually

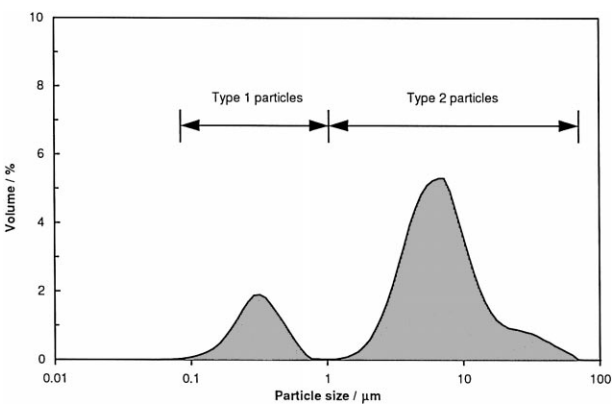

Fig. 1. Particle-size distribution of Bi-bearing oxide.

Table 2
Acid absorption value and BET specific surface area of Barton-pot oxides

Oxide type	Acid absorption value (mg H_2SO_4 per g oxide)	BET surface area ($m^2\ g^{-1}$)
Bi-bearing oxide	146	0.61
Bi-free oxide	140	0.55

have sizes of the order of several to several tens of microns [14].

The acid absorption value and BET specific surface area of the two oxides are given in Table 2. Clearly, the presence of bismuth produces no major changes in either parameter. The values are typical of those expected for a Barton-pot oxide (see Fig. 2) [15].

Examination of the Bi-bearing oxide with an electron probe microanalyzer (JEOL, Model 8900 Super Probe) revealed that the bismuth was distributed evenly throughout the oxide with no segregation.

From the above data, it is concluded that increasing the level of bismuth and lowering those of the other impurities in soft lead produces no significant changes in either the physical or the chemical properties of oxide made from this material. Since reactivity with acid provides a useful indicator of the paste-mixing attributes of a given oxide, the absence of any major differences in acid absorption between Bi-bearing and Bi-free oxides confirms that manufacturers will experience no difficulties in paste mixing on adopting this Bi-bearing oxide in their production lines.

3. Gassing behaviour of pasted electrodes

3.1. Preparation of pasted electrodes

A section of a Pb–0.09 wt.% Ca–0.4 wt.% Sn grid was embedded in epoxy resin to give a cylinder. The unsoldered end of the grid was allowed to protrude about 2 mm above the upper surface of the cylindrical mould (Fig. 3a). A polyvinyl chloride (PVC) rod, with the same diameter as the mould, was sectioned into a slice of thickness = 3 mm. A hole (diameter = 6 mm) was drilled through the centre of the PVC slice and a cylindrical paper strip was fixed to the inner wall of the hole. The PVC slice was placed on the upper surface of the electrode assembly so that the grid was located at the centre of the hole (Fig. 3a). The pastes for positive and negative electrodes were prepared from Bi-free and Bi-bearing oxides using the formulae given in Table 3. The hole in the above assembly was filled with paste and the PVC slice was then removed to give the final dimensions of the electrode, as shown in Fig. 3b.

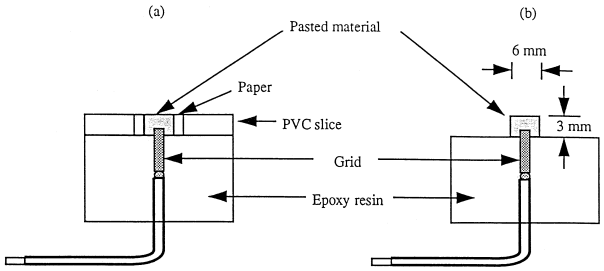

Fig. 3. Preparation of pasted electrodes for electrochemical studies.

The pasted samples were cured under conditions which promote the development of tribasic lead sulfate ($3PbO \cdot PbSO_4 \cdot H_2O = 3BS$). After curing and drying, the samples were placed in a petri dish which contained 1.070 sp. gr. H_2SO_4. Electrode formation was achieved by applying, for 20 h, a constant current of 17.7 mA per g of cured material.

3.2. Gassing measurements

The electrochemical cell used in this study is shown in Fig. 4. The pyrex cell has an H-shape with two main compartments. The cell was filled with 1.275 sp. gr. H_2SO_4. A sheet of pure lead served as the counter electrode. All potentials were measured (and are reported) with respect to a 5 M Hg/Hg_2SO_4 reference electrode.

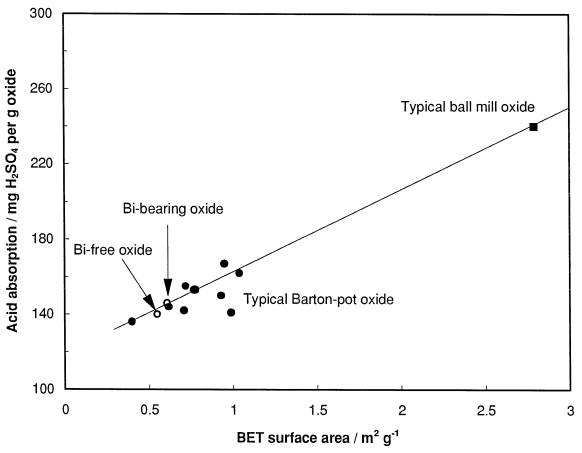

Fig. 2. Reactivity of Bi-bearing and Bi-free Barton-pot oxides. Other data are taken from Ref. [15].

Table 3
Paste formulae for positive and negative electrodes

Component	Positive electrode	Negative electrode
Leady oxide (kg)	3	3
Fibre (g)	0.9	1.8
CMC[a] (g)	7.5	–
Stearic acid (g)	–	1.8
$BaSO_4$ (g)	–	11.1
Vanisperse (g)	–	11.1
Carbon black (g)	–	6.3
1.400 sp. gr. H_2SO_4 (cm^3)	200	200
Water (cm^3)	390	330
Paste density (g cm^{-3})	4.5–4.6	4.7–4.8

[a] Carboxymethyl cellulose.

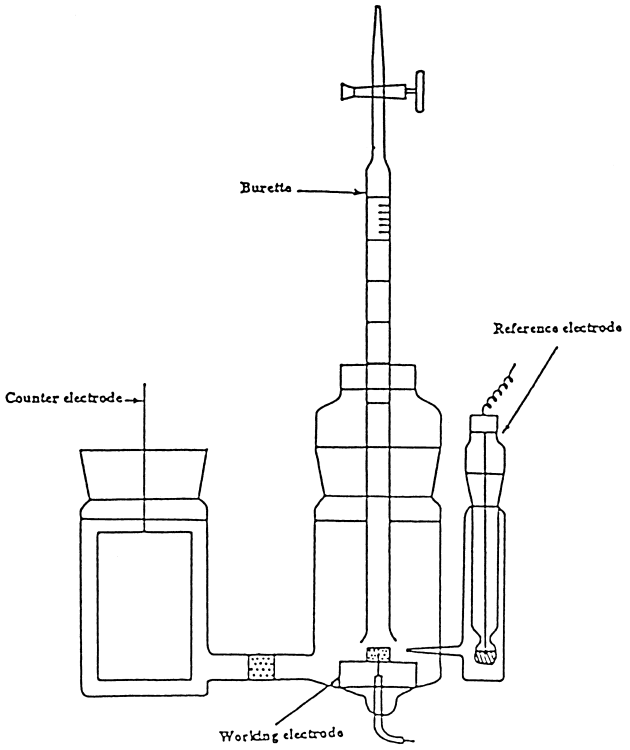

Fig. 4. Electrochemical cell used for gassing measurements.

After formation, each sample was placed in the test cell and the potential was scanned, either between −1.1 and −1.7 V or between 1.3 and 1.7 V at 5 mV s^{-1} for 20 cycles with a programmable potentiostat/galvanostat (EG &G PAR 273), prior to the respective measurement of hydrogen and oxygen evolution. With this treatment, any lead sulfate residues (due to incomplete formation and/or the chemical development of sulfation layers) will be converted, respectively, to lead or lead dioxide. For studies of both hydrogen and oxygen evolution, a potential-step technique was used and the gas produced at each potential was collected. The current density for oxygen evolution (i_{oxygen}) and hydrogen evolution ($i_{hydrogen}$) was calculated by means of the following expressions:

$$i_{oxygen} = [4FV(P_{total} - P_w)]/[10^6\, RTAt] \quad (1)$$

$$i_{hydrogen} = [2FV(P_{total} - P_w)]/[10^6\, RTAt] \quad (2)$$

where: $F = 96{,}485$ C mol^{-1}; P_{total} = total pressure (kPa) in the upper part of the burette; P_w = vapour pressure (kPa) at temperature T; V = gas volume (ml) collected in the burette; R = gas constant ($= 8.31$ J mol^{-1} K^{-1}); T = absolute temperature (K); A = electrode area (cm^2); t = electrolysis period (s). Note, two or more separate determinations of the current were undertaken at each potential. The average values are reported.

3.3. Oxygen evolution on pasted electrodes

Oxygen-evolution data for positive electrodes produced from Bi-bearing and Bi-free oxides are shown in Fig. 5. As expected, the oxygen-evolution rate increases with increase in positive potential from 1.2 to 1.7 V. There are no major differences in the rate of oxygen evolution for the two electrodes. Thus, the presence of 0.05 wt.% Bi in the oxide does not produce any undesirable increase in gassing.

As mentioned above, the Pasminco specification for soft lead increases the limits for beneficial elements, such as bismuth, to levels which can cause an improvement in battery cycle-life. By contrast, impurities such as As, Co, Cr, Ni, Sb and Te, which are harmful to VRLA batteries, are restricted to very low levels. The details of the Pasminco specification are compared in Table 4 with those of other Standards. The data demonstrate clearly that there is a marked difference of opinion world-wide on the purity required for soft lead. Moreover, many impurities have hitherto not been specified, even though some of them are known to enhance oxygen and/or hydrogen gassing (e.g., Co and Te [13]). In order to examine the effect(s) of these impurities on the gassing characteristics of lead–acid batteries, pasted electrodes were prepared from Bi-bearing oxides in which the levels of all the impurity elements (except sulfur) were increased either to the maximum (termed: 'high-impurity, Bi-bearing oxide') values specified in the British Standard 334-1982 or to medium values (i.e., 50% of each maximum level, termed: 'medium-impurity, Bi-bearing oxide'). This was achieved by blending the Bi-bearing oxide with each of the elements in powdered oxide form before paste mixing. Note, a maximum level of 10 ppm was used for any element which is not specified in the British Standard.

The oxygen-evolution rates of the positive electrodes prepared from medium- and high-impurity, Bi-bearing oxides are presented in Fig. 5. The data show clearly that increased levels of impurities in the Bi-bearing oxide produce a corresponding increase in the oxygen gassing rate at all potentials between 1.4 and 1.7 V; the increase is virtually the same for oxide blended with impurities at a medium or a high level. It is concluded that the common impurities in soft lead—but not bismuth—dominate the rate of oxygen evolution.

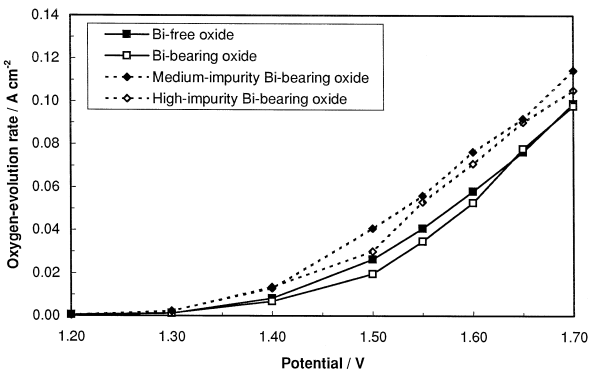

Fig. 5. Oxygen evolution on pasted electrodes prepared from oxide of different purity.

Table 4
Impurity limits (maximum ppm) in proposed Pasminco specification and other existing standards for soft lead

Element	Pasminco specification (proposed)	Existing standards			
		AS 1812-1975, Pb 99.99	ASTM B29-92, Refined pure	BS 334-1982, Type A	DIN 1719-1986, Pb 99.99
Ag	10	10	25	25	10
As	1	10	5	5	10
Ba	10	ns	ns	ns	ns
Co	1	[a]	ns	ns	ns
Cr	5	ns	ns	ns	ns
Cu	10	10	10	30	10
Fe	5	10	10	30	10
Mn	3	ns	ns	ns	ns
Mo	3	ns	ns	ns	ns
Ni	2	[a]	2	10	ns
S	10	10	ns	5	ns
Sb	1	10	5	20	10
Se	1	ns	ns	ns	ns
Te	0.3	ns	1	ns	ns
V	4	ns	ns	ns	ns

ns = Not specified.
[a] Co + Ni < 10 ppm.

3.4. Hydrogen evolution on pasted electrodes

The rate of hydrogen evolution on pasted negative electrodes prepared from different oxides is presented in Fig. 6. The results show that the hydrogen-evolution rate increases with increase in the negative-plate potential, irrespective of the nature of the starting oxide. When the potential is more positive than −1.5 V, there is little difference in the hydrogen-gassing rate on pasted electrodes made from Bi-bearing and Bi-free oxides. By contrast, at potentials more negative than −1.5 V, the hydrogen-evolution rate on pasted electrodes prepared from Bi-free oxide increases markedly in comparison with that on the electrode produced from Bi-bearing oxide.

As with the oxygen-gassing studies, the hydrogen-evolution behaviour has also been examined for pasted electrodes prepared from medium- or high-impurity, Bi-bearing oxides. The rate of hydrogen evolution increases when the level of each impurity element is raised above that specified by Pasminco for Bi-bearing oxide. Unlike the behaviour observed for oxygen gassing, however, the rate is greater for high-impurity than for medium-impurity electrodes. More importantly, appreciable hydrogen evolution occurs on both electrodes at potentials as high as −1.1 V.

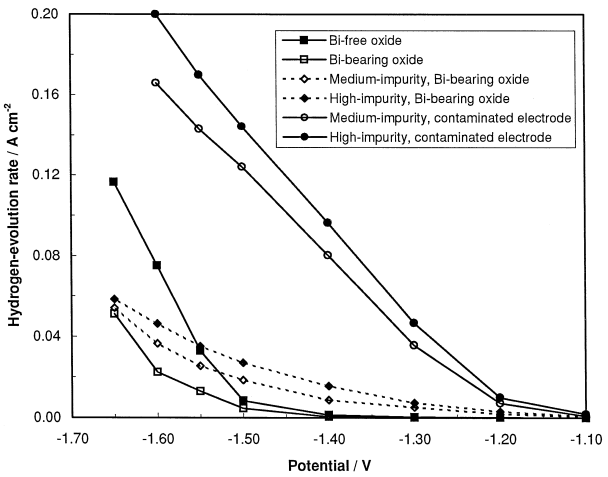

Fig. 6. Hydrogen evolution on pasted electrodes prepared from oxide of different purity.

It is well known that gassing (i.e., oxygen or hydrogen) occurs predominantly on the surface of the plate material and from the walls of the pores within the plate material. Therefore, any contamination of the surface by impurity elements is likely to affect markedly the hydrogen-gassing characteristics of the electrode if the impurities have the ability to sustain a lower hydrogen overpotential than lead. Accordingly, it is important to examine the hydrogen-gassing rates of electrodes on which various impurity elements are deposited. This situation simulates the contamination of negative plates during battery cycling—a common problem caused by the deposition of impurities that have been leached from the positive plates (i.e., from the grid alloys and/or the plate material).

After formation, negative electrodes were placed in sulfuric acid solution which contained different impurities at the maximum levels specified in the British Standard 334-1982 (see Table 5). Some elements were excluded because they either do not dissolve (Ag) or do not deposit (As, Ba, Cr) on the negative electrode. It should be noted that while molybdenum, alone, cannot be deposited from aqueous solution [16,17], it can be co-deposited in the presence of Fe, Co, or Ni.

In order to obtain a negative electrode with the same levels of impurities as that prepared from high-impurity, Bi-bearing oxide, the charge required to deposit individual elements was calculated by assuming that the current

Table 5
Charge required to deposit each impurity element

Element	Impurity levels in Bi-bearing oxide	Impurity levels specified in BS 334-1982[a]	Difference	Charge required for deposition (Ah)
Co	1	10	9	0.0032
Cu	10	30	20	0.0067
Fe	5	30	25	0.0096
Mn	3	10	7	0.0054
Mo	3	10	7	0.0031
Ni	2	10	8	0.0029
Sb	1	20	19	0.0050
Se	1	10	9	0.0024
Te	0.3	10	9.7	0.0032
V	4	10	6	0.0063
				Total = 0.0478

[a]The values in parenthesis are not specified in BS 334-1982 but were adopted in the experiments performed here.
The weight of the electrode material is ~0.4 g.

efficiency for the deposition of all elements is similar and equal to 0.1% (see Table 5). The total charge required is 0.0478 Ah. Taking this value, negative electrodes of medium– and high–impurity can be obtained by applying a current of 7.5 mA for 3.19 and 6.37 h, respectively. Note, the current efficiency for deposition is dependent upon both the inherent characteristics of each element and the concentration of the element in the plating solution. Nevertheless, at concentrations of a few ppm, the current efficiency for each element is very similar and has a very low value (i.e., 0.1%).

The negative electrodes on which elements were deposited up to the medium– and high–impurity levels are termed 'medium-impurity, contaminated electrodes' and 'high-impurity, contaminated electrodes', respectively. The gassing behaviour of these electrodes is presented in Fig. 6. As expected, the hydrogen-evolution rate increases significantly compared with that sustained by electrodes prepared from either medium- or high-impurity, Bi-bearing oxides. This is because although the total concentration of each impurity is virtually the same in a given type (medium-impurity or high-impurity) of blended or contaminated electrode, the surface concentration is considerably higher in the contaminated electrodes. The rate of hydrogen evolution is greater on the high-impurity, contaminated electrodes than on the medium-impurity, contaminated counterparts.

4. Relevance to lead–acid batteries

The above gassing behaviour of individual positive and negative electrodes prepared under various conditions will be discussed in terms of the expected combined effects of oxygen and hydrogen evolution on the performance of low-maintenance (i.e., low-antimony grid alloys) and maintenance-free (i.e., Pb–Ca–Sn grid alloys) flooded-electrolyte batteries, as well as on the performance of VRLA batteries. Obviously, at this stage, the following analysis can only serve as a qualitative guide to the performance of batteries that use the above electrodes.

4.1. Flooded-electrolyte batteries

The rates of oxygen and hydrogen evolution (logarithmic scale) during overcharging of flooded-electrolyte, lead–acid batteries at a constant voltage of 2.45 V per cell are shown in Fig. 7. For clarity, it is assumed that oxygen and hydrogen are the only side reactions which are occur-

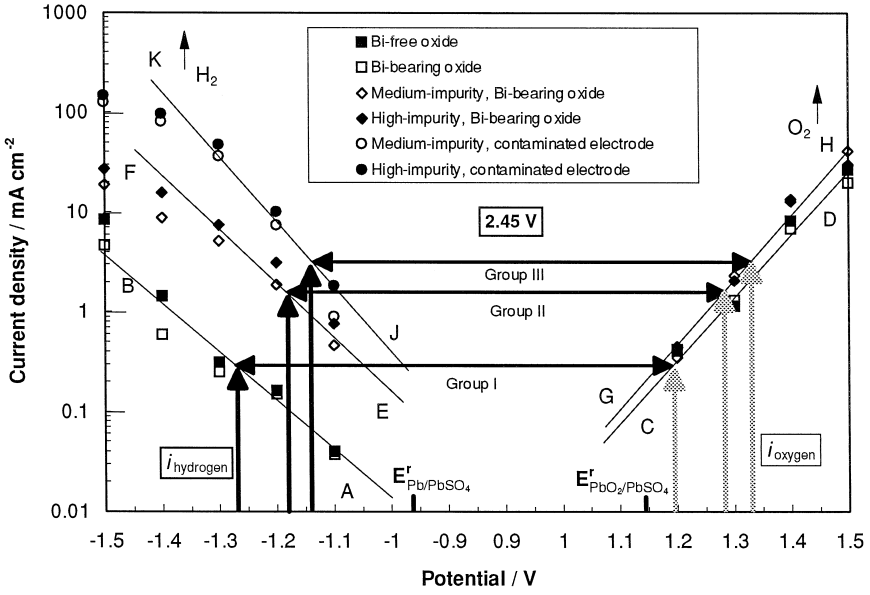

Fig. 7. Constant-voltage charging of flooded-electrolyte batteries.

ring. In addition, the batteries are classified into the following three groups:

group I: batteries with positive and negative plates produced from Bi-bearing or Bi-free oxide;

group II: batteries with positive and negative plates produced from medium- or high-impurity, Bi-bearing oxide;

group III: batteries with positive plates prepared from medium- or high-impurity, Bi-bearing oxide, and with medium- or high-impurity, contaminated negative plates also prepared from Bi-bearing oxide.

Note, the levels of impurities in the medium- or high-impurity, Bi-bearing oxide are within the values specified in the British Standard 334-1982 or are set at 5 or 10 ppm, respectively, in those cases where a value is not given.

In each battery group, the potentials of the positive and negative plates are shifted from their corresponding equilibrium values ($E^{r}_{PbO_2/PbSO_4}$ and $E^{r}_{Pb/PbSO_4}$) to such an extent that the same current flows through both polarities. For group I batteries with positive and negative plates produced from Bi-bearing or Bi-free oxide, there is no significant difference in the rate of either oxygen or hydrogen evolution over this operational voltage (see AB, CD, Fig. 7). By contrast, both rates (particularly that for hydrogen evolution) are increased in group II batteries which are made from oxide containing higher levels of impurities (cf., EF with AB, and GH with CD, Fig. 7). The hydrogen-gassing rate is further enhanced in group III batteries when the negative plate is contaminated via the deposition of impurity elements which originate either from the electrolyte or from the positive plates (cf., JK and EF, Fig. 7).

During charge–discharge cycling, it is clear that less gassing and, thereby, less water loss will be expected from group I batteries than from group II and III counterparts. Moreover, due to lower rates of oxygen and hydrogen gassing, the group I batteries will have better charging efficiency. The other important observation is that the potential of the positive plate shifts to more positive values when the gassing rate of the battery is increased. It is well established [18] that the corrosion rates of both low-antimony and Pb–Ca–Sn grids increase with increase in positive-plate potential (i.e., > 1.23 V). This indicates that in addition to the benefits of less gassing, less water loss and better charging efficiency, the batteries made from Bi-bearing or Bi-free oxide (group I) will experience less positive-grid corrosion than those produced from oxide with high impurity levels (group II) or with contaminated negative plates (group III).

The self-discharge of individual positive and negative plates in a battery is determined mainly by the amount of oxygen and hydrogen gassing that takes place under open-circuit conditions via the following reactions.

At positive plate:

$$H_2O \rightarrow 1/2O_2 + 2H^+ + 2e^- \quad (3)$$

$$PbO_2 + 2H^+ + H_2SO_4 + 2e^- \rightarrow PbSO_4 + 2H_2O \quad (4)$$

At negative plate:

$$2H^+ + 2e^- \rightarrow H_2 \quad (5)$$

$$Pb + H_2SO_4 \rightarrow PbSO_4 + 2H^+ + 2e^- \quad (6)$$

The rate of oxygen or hydrogen evolution caused by self-discharge can be estimated from the intersection of the corresponding gas-evolution curve with the equilibrium potential of the positive or negative plate (see Fig. 8). Clearly, the self-discharge at positive and negative plates will be lower in group I, than in group II and III batteries.

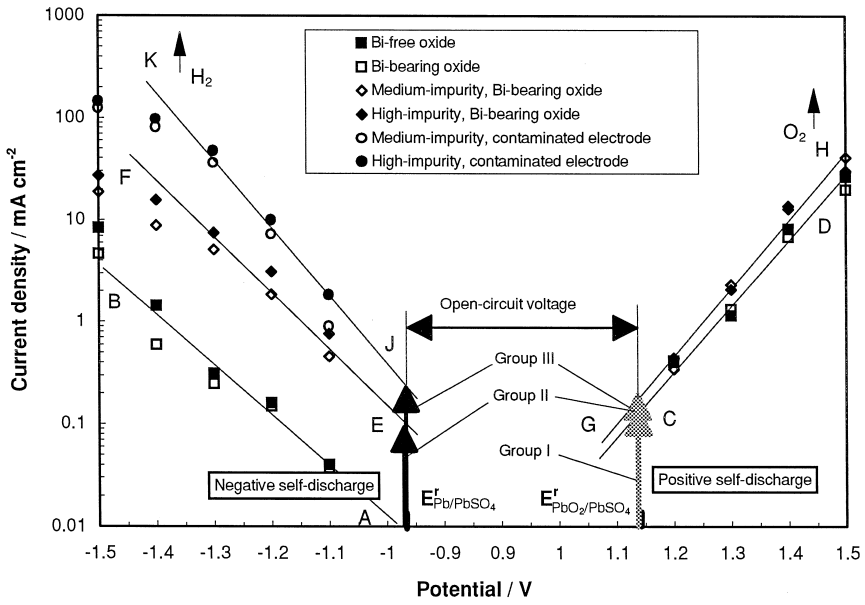

Fig. 8. Self-discharge of positive and negative plates in flooded-electrolyte battery.

The above simple relationship between the gassing current and the potentials of the positive and negative plates is, however, only an approximation. This is because other secondary reactions (i.e., grid corrosion and oxygen reduction) also occur during overcharge. The current consumed by these reactions is more important in the operation of VRLA batteries than in flooded-electrolyte counterparts.

4.2. VRLA batteries

In VRLA batteries, the situation is quite different. At the positive plates, the overcharge current is consumed mainly by oxygen evolution. Only a minor amount ($\sim 2\%$ [19]) is consumed by grid corrosion (note, oxidation of hydrogen is negligible). Nevertheless, the current associated with grid corrosion cannot be neglected (see later). Oxygen evolved from the positive plates will diffuse through either the pores of the separators or through the head space of the container to the negative plates, see Fig. 9. The oxygen is then reduced chemically via the formation of lead sulfate, i.e.,

$$Pb + 1/2O_2 + H_2SO_4 \rightarrow PbSO_4 + H_2O \quad (7)$$

Since the negative plates are simultaneously on charge, the lead sulfate is immediately reduced electrochemically to lead and the chemical balance of the cell is restored, i.e.,

$$PbSO_4 + 2H^+ + 2e^- \rightarrow Pb + H_2SO_4 \quad (8)$$

The overall 'oxygen-reduction' or 'oxygen-recombination' reaction can be expressed by:

$$1/2O_2 + 2H^+ + 2e^- \rightarrow H_2O \quad (9)$$

Consequently, the situation at the negative plate of a VRLA battery is completely different to that experienced at the negative plate of a flooded-electrolyte battery. Oxygen reduction is now the main reaction.

Given the above considerations, the current distribution in VRLA batteries prepared from Bi-bearing or Bi-free oxide has been calculated and the results, together with those for flooded-electrolyte batteries (Fig. 7), are presented in Fig. 10. The calculations are based upon the following assumptions: (i) the efficiency of oxygen reduction is 96%; (ii) the corrosion current is 2% of the overall value; (iii) the oxidation of hydrogen and battery additives (e.g., expanders, pore formers) is negligible. As with constant-voltage overcharging (2.45 V per cell) of flooded-electrolyte batteries, both the positive- and negative-plate potentials are shifted so that the same amount of current flows through both polarities, i.e., the combined current consumed by oxygen evolution and grid corrosion at the positive plate is equal to that consumed by oxygen reduction and hydrogen evolution at the negative plate. The hydrogen evolution at the negative plate balances the grid corrosion at the positive plate and any evolved oxygen that is not subsequently reduced at the negative, i.e., $i_{\text{hydrogen}} = i_{\text{corrosion}} + (i_{\text{oxygen}} - i_{\text{oxygen reduction}})$. Since the current at the negative plate is mainly associated with oxygen reduction, that remaining for hydrogen evolution is decreased. Under such conditions, the potential of the negative plate shifts towards a more positive value, i.e., towards the equilibrium value of the $Pb/PbSO_4$ couple (i.e., $E^r_{Pb/PbSO_4}$). Correspondingly, the potential of the positive plate will shift to a more positive value in order to maintain the cell voltage at 2.45 V. Thus, because there are two possible reactions at the negative plate, the potentials of the positive and negative plates in a VRLA battery will differ from those in flooded-electrolyte battery, i.e., by an amount ΔV as shown in Fig. 10.

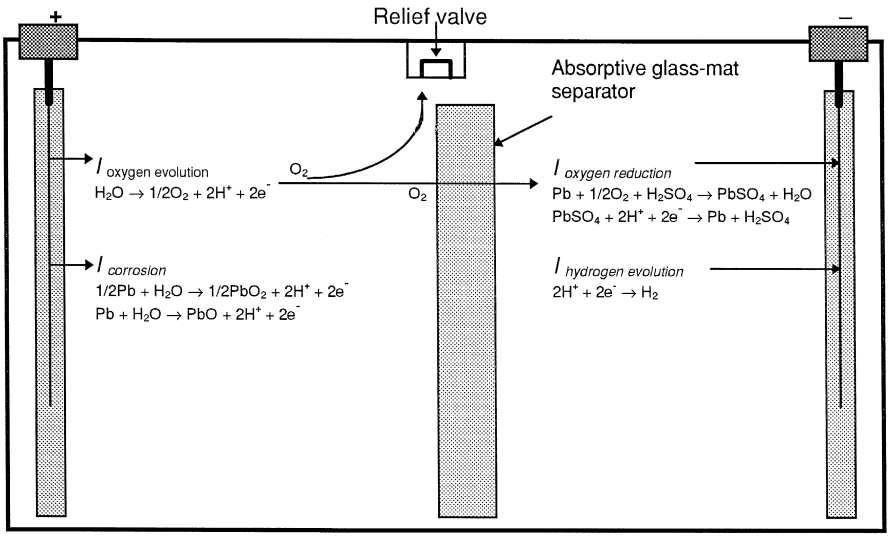

Fig. 9. Reactions which take place during recharge of a VRLA battery.

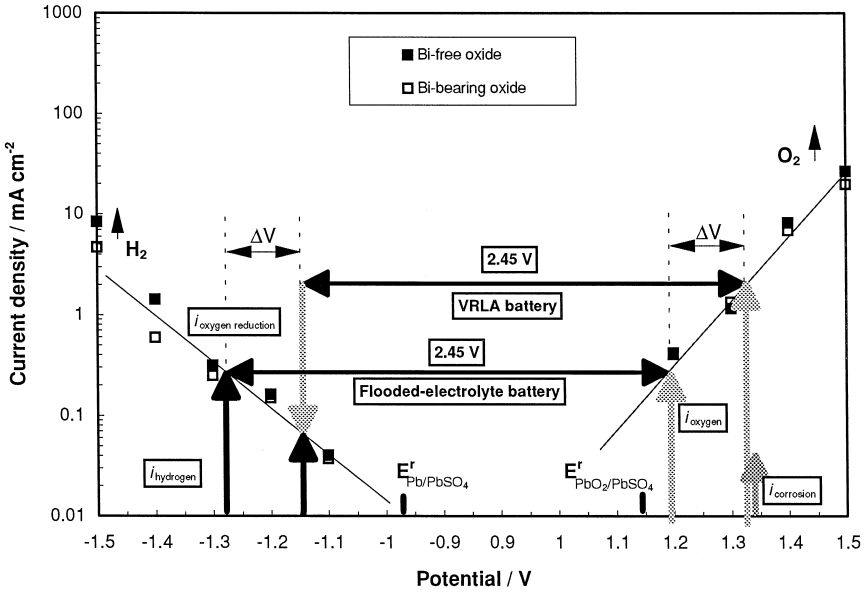

Fig. 10. Constant-voltage charging of flooded-electrolyte and VRLA batteries.

The current distribution in VRLA batteries prepared under different conditions is presented in Fig. 11. As with flooded-electrolyte designs, the group I batteries, i.e., prepared from Bi-bearing and Bi-free oxides, produce less hydrogen gassing under constant-voltage charging than group II and III counterparts and, consequently, will have less water loss and better charging efficiency. Since the potential of the positive plate in group I batteries shifts to a less-positive value than in group II and III counterparts, the group I batteries would suffer a lower rate of positive-grid corrosion even though all batteries are made from the same grid alloy. For similar plate conditions, the positive grid in a VRLA battery is more prone to corrosive attack than a grid in a flooded-electrolyte battery because the shift in positive-plate potential is larger in the former design (see Fig. 10). Such corrosion not only lowers both

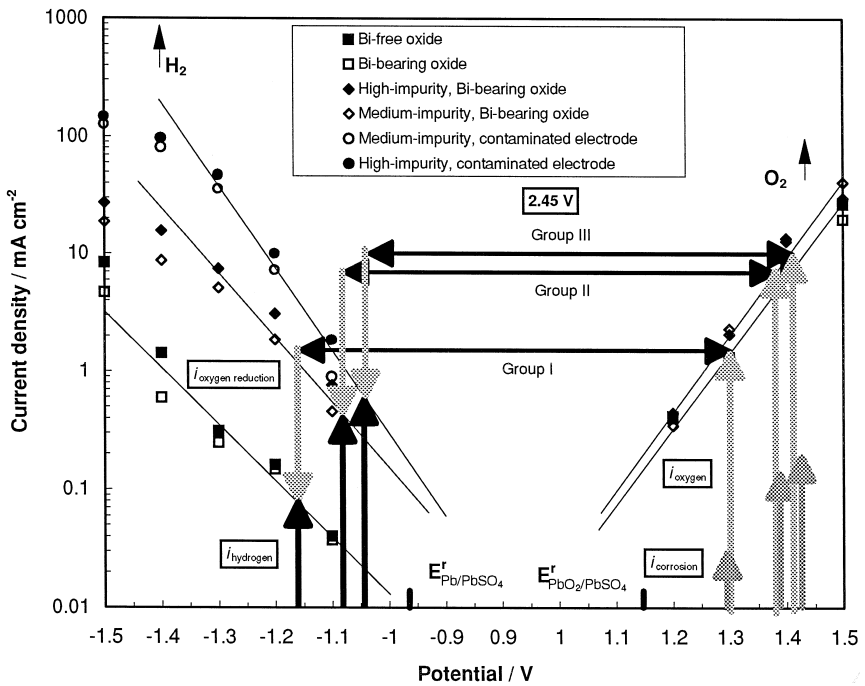

Fig. 11. Constant-voltage charging of VRLA batteries.

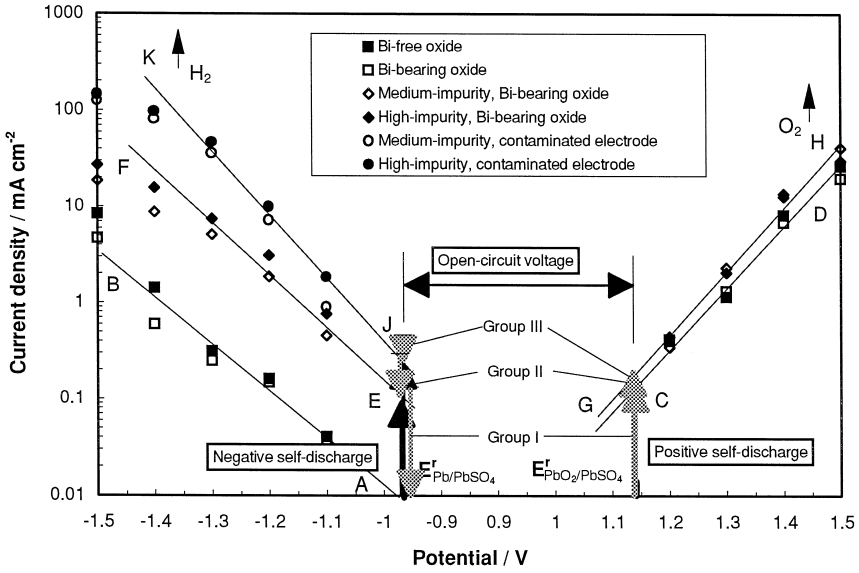

Fig. 12. Self-discharge of positive and negative plates in a VRLA battery.

the conductivity and the mechanical strength of the positive plates but also causes additional water loss via the process:

$$Pb + 2H_2O \rightarrow PbO_2 + 4H^+ + 4e^- \quad (10)$$

This water consumption is detrimental to 'acid-starved' VRLA technology because it will cause a significant loss in capacity. For example, Brecht [20] has calculated that conversion of 25% of the grid metal into PbO_2 will produce a corresponding 10% reduction in the electrolyte saturation level. If the latter falls from 95 to 85%, then a 20% or greater loss in usable capacity will occur.

For VRLA and flooded-electrolyte batteries, the self-discharge of the positive plates is basically similar, but that of the negative plates is quite different (see Fig. 12). At the negative plates in a VRLA batteries, self-discharge can proceed not only by hydrogen evolution (reactions 5 and 6) but also by oxygen reduction (see reaction 7). Thus, in a VRLA battery, the self-discharge of the negative plate depends upon the rate of self-discharge of the positive plate and upon the oxygen-recombination efficiency. In

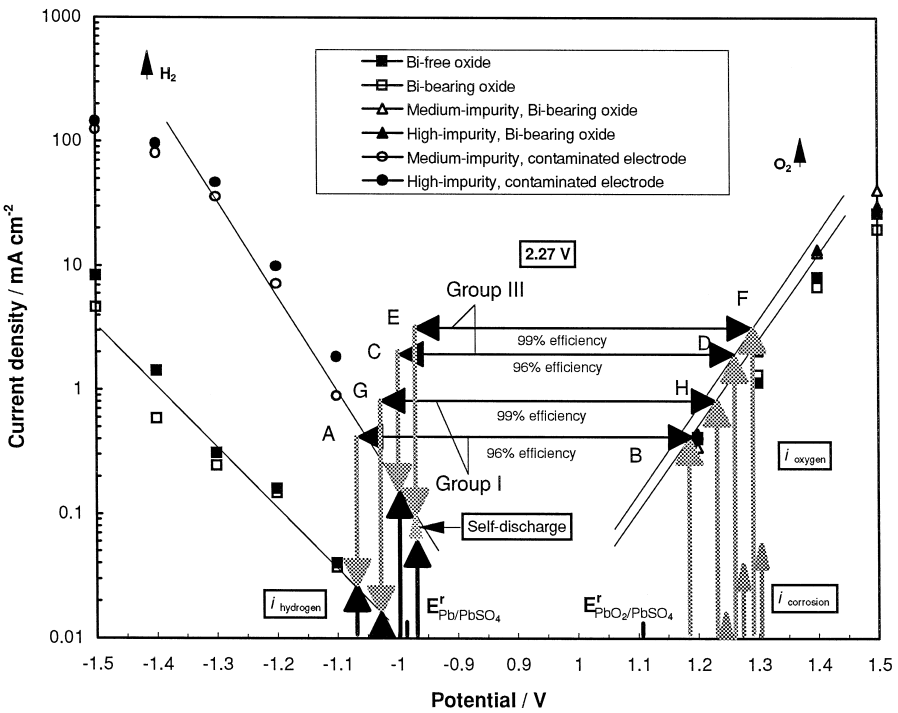

Fig. 13. Operational voltages of VRLA batteries under float conditions.

addition, the ingress of any air through the valve or container will further discharge the negative plate. As with flooded-electrolyte designs, group I batteries will undergo less self-discharge than group II and III counterparts.

As mentioned above, VRLA technology is replacing conventional, flooded-electrolyte batteries in stationary applications. Therefore, it is of interest to examine the performance of VRLA batteries prepared from oxide of different purity when used in uninterruptible power supply applications (UPS). Under such duty, the batteries are subjected continuously to constant-voltage charging ('float') at 2.27 V per cell. A comparison of the operational voltage of group I and group III batteries in UPS applications is given in Fig. 13. In the initial stages, the oxygen-reduction efficiency in both groups of batteries is assumed to be 96%. At this stage, the float current of group I batteries (i.e., both plate polarities prepared from Bi-bearing or Bi-free oxide) is lower than that of group III batteries (positive plates produced with either medium– or high–impurity, Bi-bearing oxide and contaminated negative plates produced from Bi-bearing oxide with medium or high surface contamination), cf., AB, CD in Fig. 13. Thus, group I batteries will experience less water loss and a lower rate of grid corrosion. Since group III batteries suffer more water loss and grid corrosion, the saturation level of electrolyte in these batteries will be reduced progressively to an extent that the oxygen reduction becomes very efficient (i.e., 99%). At the same time, the potential of the negative plate will shift towards more positive values so that the hydrogen-evolution current balances that of grid corrosion at the positive plate (because there is now virtually no loss of oxygen). When the potential of the negative plate moves to a value more positive than the equilibrium potential ($E^{r}_{Pb\,/\,PbSO_4}$), and the current consumed by hydrogen evolution is still higher than that consumed by grid corrosion, the difference will be taken up by self-discharge of the negative plates (see EF in Fig. 13). Thus, group III batteries may suffer negative-plate discharge during UPS duty. Jones and Feder [21] have observed this problem in some batteries after a long periods of float service. On extended service, the oxygen-reduction efficiency of group I batteries will also approach 99%. Again, the potential of the negative plate will shift towards more positive values, (i.e., towards the equilibrium value) until the current consumed by hydrogen evolution balances that consumed by grid corrosion at the counter positive plate. Given the inherent low hydrogen gassing rate, the latter condition is achieved before the negative-plate potential reaches the equilibrium value and thus self-discharge of the negative plate is prevented (cf., GH, EF in Fig. 13).

5. Conclusions

This study has highlighted the importance of setting lower limits for common impurities in the soft lead used to manufacture VRLA battery oxide. Pasted positive and negative electrodes using oxide prepared from soft lead specified by Pasminco have lower rates of oxygen and hydrogen evolution than those employing oxides in which the impurities have been raised to the maximum levels specified in the British Standard 334-1982, or to medium levels (i.e., 50% of the maximum levels). Therefore, VRLA batteries produced using the new Pasminco specification experience less water loss, better charging efficiency, and lower rates of grid corrosion and self-discharge. Furthermore, both laboratory and field trials have demonstrated that no difficulties will be encountered with existing equipment and plate-making procedures when adopting the Pasminco soft lead for oxide and battery manufacture.

Acknowledgements

The CSIRO authors are grateful to Pasminco Metals for supporting this work and for permission to publish the results.

References

[1] B. Culpin, K. Peters, N.R. Young, in: J. Thompson (Ed.), Power Sources 9, Research and Development in Non-Mechanical Electrical Power Sources, Academic Press, London, UK, 1983, p. 129.
[2] E. Nann, J. Power Sources 33 (1991) 93.
[3] M. Tsubota, S. Osumi, M. Kosai, J. Power Sources 33 (1991) 105.
[4] T. Yamada, Y. Nakazawa, Y. Tsujino, J. Power Sources 38 (1992) 123.
[5] J. Szymborski, B. Burrows, in: J. Thompson (Ed.), Power Sources 9, Research and Development in Non-Mechanical Electrical Power Sources, Academic Press, London, UK, 1983, p. 113.
[6] B. Culpin, M.W. Pilling, F.A. Fleming, J. Power Sources 24 (1988) 127.
[7] J. Kwasnik, T. Pukacka, M. Paszkiewicz, B. Szczesniak, J. Power Sources 31 (1990) 135.
[8] M. Maja, N. Penazzi, J. Power Sources 22 (1988) 1.
[9] L.T. Lam, R. De Marco, J.D. Douglas, R. Pillig, D.A.J. Rand, J. Manders, J. Power Sources 48 (1994) 113.
[10] L.T. Lam, J.D. Douglas, R. Pillig, D.A.J. Rand, J. Power Sources 48 (1994) 219.
[11] H. Sanchez, Y. Meas, L. Gonzales, M.S. Quiroz, J. Power Sources 32 (1993) 43.
[12] J.R. Pierson, C.E. Weinlein, C.E. Wright, in: D.H. Collins (Ed.), Power Sources 5, Research and Development in Non-Mechanical Electrical Power Sources, Academic Press, New York, 1975, p. 97.
[13] D.M. Rice, J.E. Manders, J. Power Sources 67 (1997) 251.
[14] G.L. Corino, R.J. Hill, A.M. Jessel, D.A.J. Rand, J.A. Wunderlich, J. Power Sources 16 (1985) 141.
[15] D.A.J Rand, L.T. Lam, The Battery Man, 34 (1992) 18–22, 24, 27, 28.
[16] D.W. Ernst, M.L. Holt, J. Electrochem. Soc. 105 (1958) 686.
[17] L.O. Case, A. Krohn, J. Electrochem. Soc. 105 (1958) 512.
[18] Proceedings of The ALABC PCL Study Group's First Meeting, Lower Beeding, West Sussex, UK, 23–24, September 1993, p. 58.
[19] J. Mrha, K. Micka, J. Jindra, M. Musilova, J. Power Sources 27 (1989) 91.
[20] W.B. Brecht, Batteries Int. 20 (1994) 40.
[21] W.E.M. Jones, D.O. Feder, Proc. TELESCON '97, Budapest, Hungary, 1997, pp. 295–303.